Phonon Modes and Exciton-Phonon Interactions in $CsPbCl_3$ Single Nanocrystals

Victor Guilloux[1], Thierry Barisien[1], Frédérick Bernardot[1], Mathieu Bernard[1], Florent Margaillan[1], Silbé Majrab[1], Ingrid Stenger[2], Emmanuel Lhuillier[1], Christophe Testelin[1], Maria Chamarro[1], Laurent Legrand[1] *

[1] Sorbonne Université, CNRS, Institut des NanoSciences de Paris, 4 Place Jussieu, F-75005 Paris, France.

[2] Université Paris-Saclay, UVSQ, CNRS, GEMaC, F-78000 Versailles, France.

Micro-photoluminescence measurements have been performed on single cubic-shaped $CsPbCl_3$ nanocrystals (NCs) with side lengths of nearly twice the Bohr diameter, i.e. in the intermediate confinement regime. We observed two peaks, linearly polarized and spectrally separated by 1 to 3 meV associated to the bright states of the exciton fine structure. We took advantage of these emission polarization properties to track the energy and the linewidth broadening of individual peaks with increasing temperature. Two regimes exist in the broadening of emission peaks, at low and high temperature, dominated respectively by acoustic or longitudinal optical phonons couplings. We deduce the respective strengths of the interactions. We also measured micro-Raman spectra of an ensemble of $CsPbCl_3$ NCs. The energy of the mean optical phonon responsible for the high temperature broadening of the emission peaks is in good agreement with the highlighted longitudinal phonon modes observed in the Raman spectra. Finally, we compare our results to previous experimental works done on other lead halide perovskites emitting at lower energy.

Keywords: perovskite nanocrystals, $CsPbCl_3$, acoustic phonons, optical phonons, exciton-phonon couplings, single object emission, quantum dots.

* Corresponding author.
E-mail address: laurent.legrand@insp.jussieu.fr (L. Legrand).

1. Introduction

All-inorganic halide perovskite nanocrystals (NCs) attract great attention due to their exceptional optical properties since their first synthesis [1]. They are considered as a new generation of promising semiconductor candidates for a wide variety of optoelectronic technologies such as light-emitting diodes [2,3], lasing devices [4-6], photo-detectors [7-10] or also for photovoltaic solar cells [11]. Among these materials whose emission can be easily tuned from near-infrared to violet by changing the composition and/or the NCs size, $CsPbCl_3$ possesses the widest bandgap energy [12,13]. In the context of the development of short-wavelength light-emitting diodes, this Cl-based perovskite appears as an ideal emitter for fabricating efficient ultrapure blue LEDs [14].

In this work, we address the exciton-phonon interaction in a single $CsPbCl_3$ NC, inside which we highlight optical phonon modes. The temperature evolution of the photoluminescence (PL) and its broadening are measured for the first time at the single NC scale in this compound. In particular, this knowledge is essential to control the purity of the blue emission. The spectral lines in the emission are selected thanks to their polarization properties. This study provides a better understanding of the processes at work in the context of the exciton-phonon interaction in a high-energy emitting material with high applicative potential in optoelectronics and confirms general trends already observed in other lower-energy emitting halide perovskites [15-24].

2. Materials and methods

Perovskite $CsPbCl_3$ NCs are grown by using a previously described method [1].

The NCs have been characterized by TEM imaging. The NCS have a cubic shape and their typical average side length is close to 8 nm, twice the Bohr diameter value of 3.4 nm (Fig. 1). A low dilute NC solution was drop-cast onto a copper grid covered with an amorphous carbon film. The grid was degassed overnight under secondary vacuum. Imaging was conducted using a JEOL 2010 transmission electron microscope operated at 200 kV.

Micro-photoluminescence (μ-PL) experiments were performed on highly diluted phases drop-cast on a glass slide, as a function of temperature in order to explore the response of individual $CsPbCl_3$ NCs. We used a frequency doubled picosecond Ti:Sapphire laser operating at 82 MHz and tuned in the range 380–400 nm *ie* in the 3.10-3.27 eV energy range. The average excitation

powers are a few μW with a spot diameter close to 1.5 μm. The excitation laser beam is focused using a microscope objective with NA = 0.6. The samples are mounted on the cold finger of a cryostat (Oxford Instruments) designed to compensate for thermal expansion and to maintain the spatial position of the spot as temperature is varied. The luminescence, collected with the same objective attached to a three-axes piezo stage to finely scan the sample spatially, is analyzed in an ACTON SP2760i Roper Scientific-Princeton Instruments spectrometer coupled to a nitrogen-cooled SPEC10 (RS-PI) CCD camera, with an overall spectral resolution of ~ 50 μeV ($\delta\lambda \sim 7$ pm) [25]. Polarization measurements are performed by adding a motorized half-wave plate followed by a linear polarizer in front of the spectrometer entrance; the direction of the polarizer is parallel to the grating grooves to optimize the spectrometer response.

Micro-Raman spectroscopy was performed using a HORIBA Jobin-Yvon Labram HR800 system using the 514.5 nm excitation wavelength of an Ar^+ laser with a power kept below 2 mW. Measurements were conducted while temperature was monitored into a liquid nitrogen cooled Linkam cryostat.

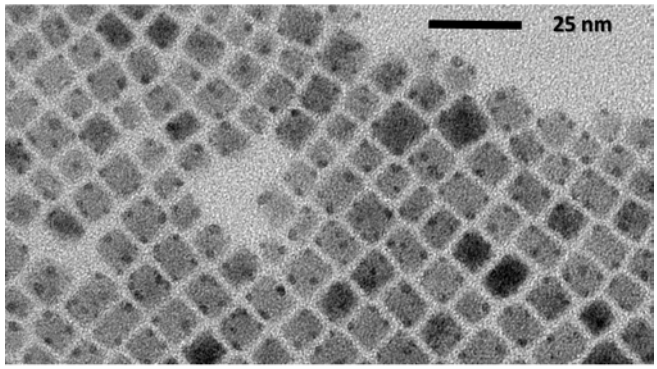

Fig. 1. TEM image of the $CsPbCl_3$ NCS addressed in this work.

3. Results and discussions

The vast majority of measured NCs shows two peaks, or doublets, with Lorentzian profiles. In very few cases a set of three lines, triplets, is observed. Each spectral component of the doublets has a linewidth in the range 0.5-1 meV at 5 K and the spacing between the two peaks varies from 1 to 3 meV. By rotating the half-wave plate of the set-up, one obtains polar diagrams for a single NC, thanks to the stability of its emission.

Figure 2(a) presents such a single NC doublet. This chosen example corresponds to a splitting of 1.47 meV between the doublet components, a value which is close to the average of the observed splittings. The polar diagram in Fig. 2(b) shows that the two peaks have linear and

crossed polarizations. Similar observations, linearly polarized doublets or triplets in the μ-PL, were made in other Pb-halide NCs [15-17,22,26-32]. These doublets or triplets are associated to the splitted exciton fine structure due to an interplay of the electron-hole exchange interaction, the crystal field and the level of shape anisotropy [33,34].

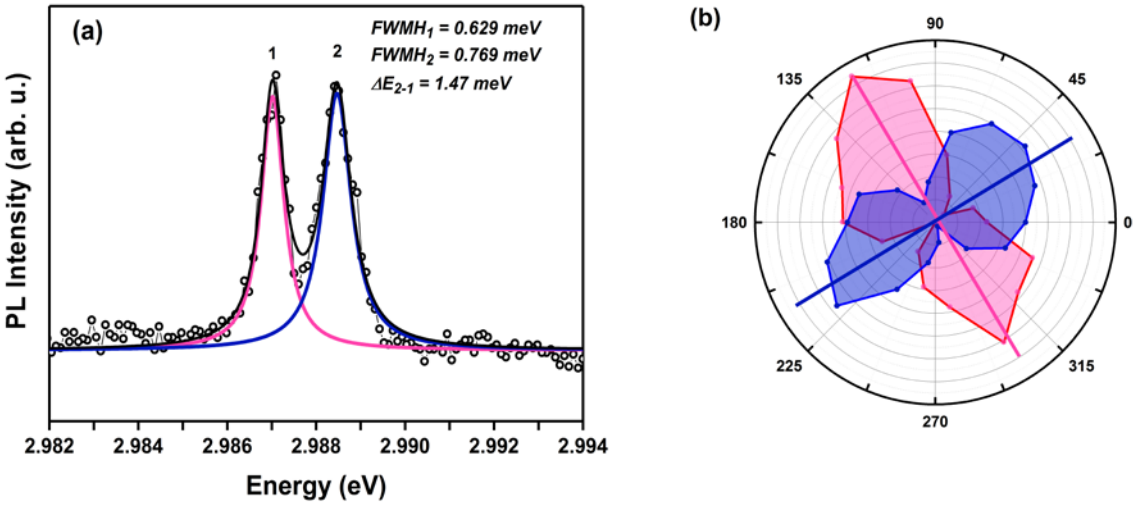

Fig. 2. μ-PL of an individual $CsPbCl_3$ NC obtained at 6 K. (a) Spectrum of a doublet. Experimental data were fitted with two single Lorentzian peaks (pink and blue). The black line is the total fit. The splitting in the EFS is here 1.47 meV. (b) Polarization diagram of the doublet. Pink and blue polarization diagrams correspond to each of the two peaks of the μ-PL spectrum.

Figure 3(a) shows the μ-PL spectrum of a single $CsPbCl_3$ NC on a larger energy domain as compared to the spectrum given in Fig. 2(a). We highlight the presence of phonon replicas since the energy shifts of the observed peaks with respect to the main excitonic line of the doublet is in good agreement with known Raman scattering $CsPbCl_3$ bulk frequencies [35-37]. As TO phonons do not couple through Fröhlich interaction with charges in such a polar system, only LO phonons replicas appear [38]. TOi (i = 1 to 3) modes as doublets have been moreover observed in bulk $CsPbCl_3$ [35,36]. We identified the longitudinal phonon replicas corresponding to LO_1, $E_{LO1} \sim 14.2$ meV, and to LO_2 with a mean energy close to 25 meV. More clearly than for LO_1 replica, this latter appears as a doublet with an energy splitting of 2 meV exactly as for the exciton doublet shown here. We therefore clearly evidence the existence of a fine-structure splitting in the LO replicas as well. This feature has been nicely evidenced recently in $CsPbBr_3$ NCs by the group of Kanemitsu [22].

We measured the micro-Raman spectrum of $CsPbCl_3$ NCs excited with a continuous excitation at 514.5 nm (2.41 eV) at different temperatures in the range 110-170 K, as seen in Fig. 3(b). The LO_2 mode is observed at 200 cm^{-1} *ie* ~ 25 meV in good agreement with the μ-PL

measurements. The LO_1 modes expected at ~ 14 meV *ie* ~ 115 cm^{-1} is covered by the TO_3 modes [35]. The inset of Fig. 3(b) shows that the Raman shifts of the three TO doublets (4, 6.5) meV, (8.9, 11.1) meV and (13.6, 15) meV (values at the lowest temperature) are almost temperature independent in the explored temperature domain, with nevertheless a small redshift of the highest frequency for the TO_2 doublet and the lowest one of the TO_1 modes within the experimental accuracy.

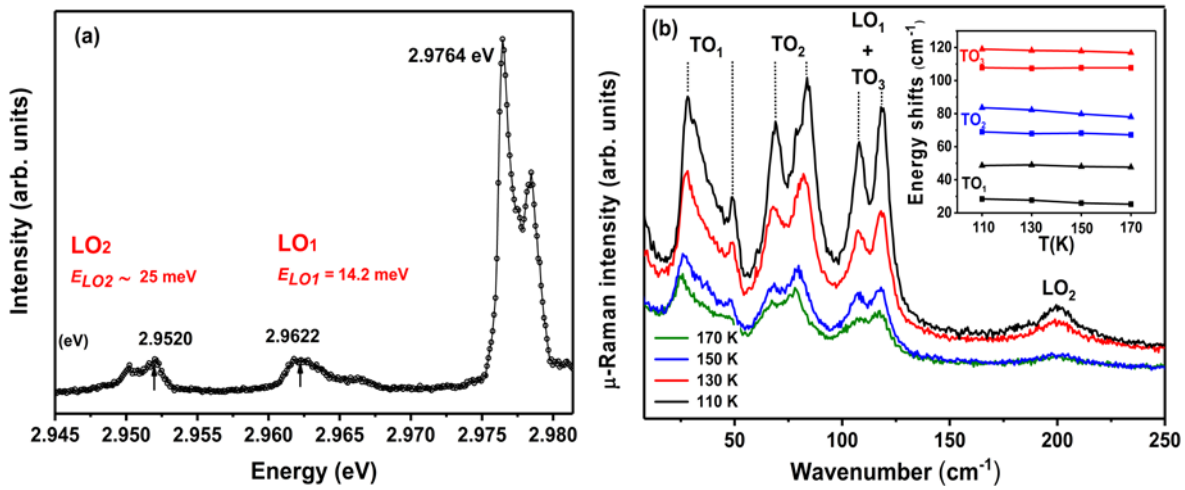

Fig. 3. (a) μ–PL spectrum at 5 K of an excitonic doublet (splitting of 2 meV) and LO phonon replicas of $CsPbCl_3$. The energies of clearly appearing structures are also indicated. The energies of the LO phonons observed are given. The energy reference is the one of the main excitonic line in this doublet. (b) Micro-Raman spectra as a function of temperature with a continuous excitation at 514.5 nm. The inset shows the weak dependences of the Raman shifts with temperature (100 cm^{-1} corresponds to ≈ 12.4 meV).

To address the exciton-phonon coupling in single $CsPbCl_3$ NCs, we take advantage of the doublet-polarization properties to follow the temperature dependence of a single homogeneous PL linewidth for several single NCs observed at 5 K. The full width at half maximum (FWHM) of these μ–PL lines has been extracted from a Lorentzian fit of the highest intensity polarized line in a doublet, carefully selected after analysis of the polarization diagrams.

To ensure that the line of a given single NC was unambiguously followed in temperature, we verified that the temperature dependence of the energy peaks of each μ–PL line evolves monotonously and with the same slope, as seen in Fig. 4 for four doublets [39].

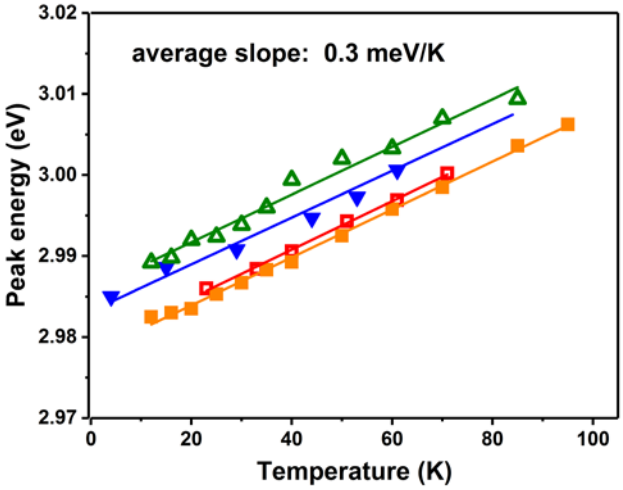

Fig. 4. Temperature dependence of the energy of the NC excitonic transitions observed in μ-PL. Each symbol is associated to a given component within the fine structure of the four observed doublets. We find an average value of the slope $\alpha_{aver.} \approx 0.3$ meV/K.

A blue-shift in energy with respect to the bulk is observed for each line. The slope measured here, $\alpha_{aver.} \sim 0.3$ meV/K, is close to the one previously determined in $CsPbBr_3$ NCs [17], which indicates a similar influence of the temperature on the lattice deformation and therefore on the energy gap.

Fig. 5 gathers the temperature dependence of the linewidth, $\Gamma(T)$, for the selected linearly polarized lines of four doublets. The broadening with temperature is modeled using the expression

$$\Gamma(T) = \Gamma_0 + A_{ac}T + B_{LO}n_{LO}(T) \quad (1)$$

where Γ_0 is a residual homogeneous temperature independent linewidth, including mainly spectral diffusion. The second term, with the A_{ac} constant, represents the homogeneous broadening resulting from charge-acoustic phonons scattering; the third one with the Fröhlich B_{LO} constant involves LO phonons [40,41]. $n_{LO}(T) = \left[\exp\left(\frac{E_{LO}}{k_B T}\right) - 1\right]^{-1}$ is the Bose-Einstein occupation number for the optical phonons, k_B is the Boltzmann constant, and E_{LO} is an average representative energy for the LO phonons [42,43]. We underline that Eq. (1) was used to fit the set of all $\Gamma(T)$ data of the four lines as a single data set in order to get a better statistics and to highlight an average behavior of the measured broadening.

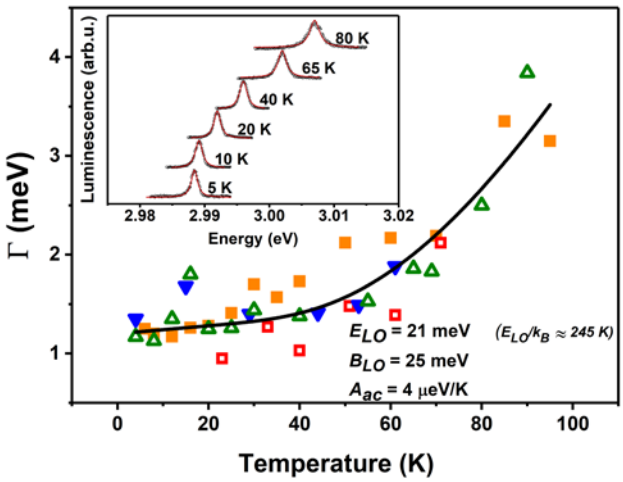

Fig. 5. Evolution with temperature of the linewidth of four selectively detected linearly polarized lines corresponding to four different NCs, which are distinguished by different symbols (the same as in Fig. 4). The fit (from Eq. (1)) is obtained when considering the four sets of data as a unique one. The inset shows the temperature evolution of one of the selected lines.

Compounds	**Samples type**	A_{ac} **(μeV/K)**	B_{LO} **(meV)**	E_{LO} **(meV)**	**References**
$FAPbBr_3$	single nanocrystals	5 ± 5	52	15.2	[16]
	polycrystalline thin films	0*	61 ± 7	15.3 ± 1.4	[20]
$CsPbBr_3$	single nanocrystals	8 ± 3	42 ± 13	16	[17]
	Micro/nanowires ensembles	0*	66	19	[24]
	nanocrystals ensembles	8.9	~ 100	~ 18	[18]
	single crystal	32	41.7	22.2	[21]
$MAPbBr_3$	polycrystalline thin films	0*	58 ± 2	~ 15	[20]
$FAPbI_3$	polycrystalline thin films	0*	40 ± 5	11.5 ± 1.2	[20]
	single nanocrystals	< 5	27	10.5 ± 0.8	[15]
$MAPbI_3$	single crystal	0*	12 ± 2	4.2 ± 0.8	[19]
	single crystals	93.5 ± 20.5	57 ± 22	16.1 ± 3.4	[23]
	polycrystalline thin films	0*	40 ± 2	~ 11	[20]
$CsPbCl_3$	single nanocrystals	4 ± 1.5	25 ± 2	21	This work

Table 1

MA stands for Methylammonium CH_3NH_3 and FA for Formamidinium $HC(NH_2)_2$. Parameters obtained when fitting the temperature emission linewidth broadening of different organic and inorganic perovskite materials under several forms, using the expression $\Gamma(T) = \Gamma_0 + A_{ac}T + B_{LO}n_{LO}(T)$ as in this work. The asterisk after the "0" in the third column indicates that this parameter has been set to zero for adjustments. In [20], measurements for MA compounds are done above 80 K. In [23], data are photocurrents measurements till 80 K.

In our experiments, as previously observed in halide perovskite materials, the exciton-LO phonons coupling appears more important as compared to the acoustic phonon coupling [15-22]. The linear part due to acoustic phonons scattering is nevertheless clearly evidenced at least

in the 5K-100K temperature domain. The coupling constants obtained from the best unique fit are $A_{ac} \sim 4$ μeV/K and $B_{LO} \sim 25$ meV, using 21 meV or 170 cm^{-1} for E_{LO} ($E_{LO}/k_B = 245$ K). The residual broadening contribution Γ_0 is close to 1.2 meV. This is higher than for $CsPbBr_3$ NCs (0.4 meV) [17]. This contribution is attributed to spectral diffusion during μ-PL measurements due to the appearance of a fluctuating charge distribution with photoexcitation.

The A_{ac} value is comparable to those which are obtained in general in organic or inorganic perovskites under several forms, as seen in Table 1 [15-21,23,24]. The E_{LO} value used here for $CsPbCl_3$ appears to stand between the values of the LO_1 (14 meV) and LO_2 (~ 25 meV) phonon energies phonon energies observed on the main phonon replicas of the μ-PL measurements presented in Fig. 3(a).

For perovskite materials, whether measured on single NCs, ensembles or even bulk materials, there is generally a good agreement between the LO phonon modes energies obtained by adjustment of the temperature linewidth broadenings and the energies measured through PL experiments or calculated for LO modes distribution directly. For example, phonon modes energies compatible with the temperature broadening of the emission lines have been observed in μ–PL experiments in the hybrid materials $FAPbI_3$ single NCs [16] or observed and computed in $MAPbI_3$ single crystal [19,44]. That is why we underline that in all-inorganic or hybrid perovskites the determination of relevant LO phonon energies *via* the measurement of the temperature dependence of line broadening in μ-PL or even of NCs sets constitutes a reliable and powerful tool. The LO energies are mainly assigned to modes related to internal vibrations of the Pb-halide network [22,45]. As seen in Table 1, the Fröhlich B_{LO} constant measured here in $CsPbCl_3$ as well as those determined in hybrid or all inorganic perovskite materials are almost all of the same order of magnitude, which reflects the polar characteristics of the Pb-halide bonds and the overall ionic character of these materials.

If we extrapolate to room temperature the fit used in Fig. 5, the obtained μ–PL linewidth for a $CsPbCl_3$ NC is of the order of 20 meV, which is in good agreement with the already considered $CsPbBr_3$ case [17].

4. Conclusions

We have characterized exciton-phonon coupling from 5 to 100 K, in single $CsPbCl_3$ NCs. We have identified optical phonons, with energies in good agreement with the micro-Raman

experiments we performed and with previous works of other groups on bulk $CsPbCl_3$. We deduced the acoustic and optical constants of the exciton-phonon couplings. The extrapolation of our single NC linewidth measurements up to room temperature leads to a linewidth of the order of 20 meV, comparable to the case of equivalent Br-based materials. This value sets a characteristic limit to the spectral width for short-wavelength light emitting diodes using this material at ambient temperature. Further investigations are required to explain the residual broadening contribution attributed to spectral diffusion usually due to the electrostatic environment of the NC.

Declaration of competing interest

The authors declare that they have no known competing financial interests or personal relationships that could have appeared to influence the work reported in this paper.

Acknowledgments

Authors thank Xiang Zhen Xu for performing the TEM imaging. This work was financially supported by the French National Research Agency (ANR IPER- Nano2, ANR- 18-CE30). EL thanks the support ERC starting grant blackQD (n°756225).

References

[1] L. Protesescu, S. Yakunin, M. I. Bodnarchuk, F. Krieg, R. Caputo, C. H. Hendon, R. X. Yang, A. Walsh, and M. V. Kovalenko, Nano Lett. 15 (2015) 3692.

[2] Z-K Tan, R. S. Moghaddam, M. L. Lai, P. Docampo, R. Higler, F. Descher M. Price, A. Sadhanala, L. M. Pazos, D. Credgington, F. Hanusch, T. Bein, H. J. Saith, and R. H. Friend, Nat. Nanotechnol. 9 (2014) 687-692.

[3] K. Lin, J. Xing, L. N. Quan, F. P. G. de Arquer, X. W. Gong J. X. Lu, L. Q. Xie, W. J. Zhao, D. Zhang, C. Z. Yan, W. Q. Li, X. Y. Liu, Y. Lu, J. Kirman, E. H. Sargent, Q. H. Xiong, and Z. H. Wei., Nature 562 (7726) (2018) 245-248.

[4] S. D. Stranks, and H. J. Snaith, Nat. Nanotechnol. 10 (2015) 391-402.

[5] H. M. Zhu, Y. P. Fu, F. Meng, X. X. Wu, Z. Z. Gong, Q. Ding, M. V. Gustafsson, M. T. Trinh, S. Jin, and X. Y. Zhu, Nat. Mater. 14(6) (2015) 636-U115.

[6] G. Xing, N. Mathews, S. S. Lim, N. Yantara, X. Liu, D. Sabba, M. Grätzel, S. Mhaisalkar, and T. C. Sum, Nat. Mater. 13 (2014) 476-480.

[7] P. Ramasamy, D.-H. Lim, B. Kim, S.-H. Lee, M.-S. Lee, and J.-S. Lee, Chem. Commun. 52 (2016) 2067.

[8] L.T. Dou, Y. Yang, J. B. You, Z. R. Jong, W. H. Chang, G. Li, and Y. Yang, Nat. Commun. 5 (2014) 5404.

[9] Y. J. Fang, Q. F. Dong, Y. C. Shao, Y. B. Yuan, and J. S. Huang, Nature Photon. 9(10) (2015) 679-686.

[10] W. J. Mir, C. Livache, N. Goubet, B. Martinez, A. Jagtap, A. Chu, N. Coutard, H. Cruguel, T. Barisien, S. Ithurria, A. Nag, B. Dubertret, A. Ouerghi, M. G. Silly, E. Lhuillier, Appl. Phys. Lett. 112 (2018) 113503.

[11] M. V. Kovalenko, L. Protesescu, and M. Bodnarchuk, Science 358 (2017) 745.

[12] M. Baranowski, P. Plochocka, R. Su, L. Legrand, T. Barisien, F. Bernardot, Q. Xiong, C. Testelin, and M. Chamarro, Photon. Res. 8 (2020) A50-A55.

[13] T Hayashi, T Kobayashi, M Iwanaga, and M Watanabe., J. of Lum. 95 (2001) 255–259.

[14] C. Zhang, Q. wan, L. K. Ono, Y. Liu, W. Zheng, Q. Zhang, M. Liu, L. Kong, L. Li, and Y. Qi, ACS Energy Lett. 6 (2021) 3545.

[15] M. Fu, P. Tamarat, J.-B. Trebbia, M. I. Bodnarchuk, , M. V. Kovalenko, J. Even, and B. Lounis, Nat. Commun. 9 (2018) 3318.

[16] P. Tamarat, M. L. Bodnarchuk, J.-B. Trebbia, R. Erni, M. V. Kovalenko, J. Even, B. Lounis, Nat. Mater. 18 (2019) 717–724.

[17] J. Ramade, L. M. Andriambariarijaona, V. Steinmetz, N. Goubet, L. Legrand, T. Barisien, F. Bernardot, C. Testelin, E. Lhuillier, A. Bramati, and M. Chamarro, Appl. Phys. Lett. 112 (2018) 072104.

[18] A. Shinde, R. Gahlaut, and S. Mahamuni, J. Phys. Chem. C 121 (2017) 14872.

[19] H. Diab, G. Trippé-Allard, F. Lédée, K. Jemli, C. Vilar, G. Bouchez, V.L.R. Jacques, A. Tejeda, J. Even, J.-S. Lauret, E. Deleporte, and D. Garrot, J. Phys. Chem. Lett. 7 (2016) 5093.

[20] A.D. Wright, C. Verdi, R. L. Milot, G. E. Eperon, M. A. Pérez-Osorio, H. J. Snaith, F. Giustino, M. B. Johnston, and L. M. Herz, Nat. Commun. 7 (2016) 11755.

[21] X. Zhou, and Z. Zhang, AIP Advances 10 (2020) 125015.

[22] K. Cho, H. Tahara, T. Yamada, H. Suzuura, T. Tadano, R. Sato, M. Saruyama, H. Hirori, T. Teranishi, and Y. Kanemitsu, Nano Lett. 22 (2022) 7674-7681.

[23] L. Q. Phuong, Y. Nakaike, A. Wakamiya, and Y. Kanemitsu, J. Phys. Chem. Lett. 7 (2016) 4905-4910.

[24] Z. Zhao, M. Zhong, W. Zhou, Y. Peng, Y. Yin, D. Tang, and B. Zou, J. Phys. Chem. C 123 (2019) 25349-25358.

[25] T. Barisien, L. Legrand, Z. Mu, and S. Hameau, Phys. Chem. Chem. Phys. 18 (2016) 12928.

[26] O. Pfingsten, J. Klein, L. Protesescu, M. I. Bodnarchuk, M. V. Kovalenko, and G. Bacher, Nano Lett. 18 (2018) 4440.

[27] L. Liu, F. Pevere, F. Zhang, H. Zhong, and I. Sychugov, Phys.Rev. B 100 (2019) 195430.

[28] L. Liu, R. Zhao, C. Xiao, F. Zhang, F. Pevere, K. Shi, H. Huang, H. Zhong, and I. Sychugov, J. Phys. Chem. Lett. 10 (2019) 5451.

[29] C. Yin, L. Chen, N. Song, Y. Lv, F. Hu, C. Sun, W. W. Yu, C. Zhang, X. Wang, Y. Zhang, and M. Xiao, Phys. Rev. Lett. 119 (2017) 026401.

[30] P. Tamarat, L. Hou, J.-P. Trebia, A. Swarnkar, L. Biadala, Y. Louyer, M. I. Bodnarchuk, M. V. Kovalenko, J. Even, and B. Lounis, Nat. Commun. 11 (2020) 6001.

[31] M. Fu, P. Tamarat, H. Huang, J. Even, A. L. Rogach, and B. Lounis, Nano Lett. 17 (2017) 2895.

[32] J. Ramade, L. M. Andriambariarijaona, V. Steinmetz, N. Goubet, L. Legrand, T. Barisien, F. Bernardot, C. Testelin, E. Lhuillier, A. Bramati, and M. Chamarro, Nanoscale 10 (2018) 6393-6401.

[33] A. Ghribi, S. Ben Radhia, K. Boujdaria, L. Legrand; T. Barisien, M. Chamarro, and C. Testelin, Phys. Rev. Materials 6 (2022) 106001.

[34] R. Ben Aich, S. Ben Radhia, K. Boujdaria, M. Chamarro, and C. Testelin, J. Phys. Chem. Lett. 11 (2020) 808.

[35] D. M. Calistru, L. Mihut, S. Lefrant, and I. Baltog, J. Appl. Phys. 82 (1997) 5391-5395.

[36] M. Liao, B. Shan, and M. Li, J. Phys. Chem. Lett. 10 (2019) 1217-1225.

[37] S. Hirotsu, Physics Letters 41 (1972) 55-56.

[38] J. Singh, 'Electronic and Optoelectronic Properties', Chapter 6, Cambridge Univeristy Press

of Semiconductor Structures, 2007.

[39] Y.P. Varshni, Physica 34 (1967) 149.

[40] T. Itoh and M. Furumiya, J. Lumin. 48–49 (1991) 704.

[41] S. Rudin, T.L. Reinecke, and B. Segall, Phys. Rev. B 42 (1990) 11218.

[42] P.Y. Yu and M. Cardona, *Fundamentals of Semiconductors Physics and Materials Properties* (Springer, Berlin, 2003).

[43] X.B. Zhang, T. Taliercio, S. Kolliakos, and P. Lefebvre, J. Phys. Condens. Matter 13(2001) 7053.

[44] A.M.A. Leguy, A.R. Goni, J. M. Frost, J. Skelton, F. Brivio, X. Rodriguez-Martinez, O. J. Weber, A. Pallipurath, M. I. Alonso, M. Campoy-Quiles, M. T. Weller, J. Nelson, A. Walsh, and P. R. F. Barnes, Phys. Chem. Chem. Phys. 18 (2016) 27051-27066.

[45] M. A. Pérez-Osorio, R. L. Milot, M. R. Filip, J. B. Patel, L. M. Herz, M. B. Johnston, and F. Giustino, J. Phys. Chem. C 119 (2015) 25703.